Journal of Hazardous Materials 496 (2025) 139202

Contents lists available at ScienceDirect

Journal of Hazardous Materials

journal homepage: www.elsevier.com/locate/jhazmat

Comparison of the toxicity/carcinogenicity of regulated and unregulated mineral fibres using the Fibre Potential Toxicity Index (FPTI)

Alessandro F. Gualtieri [a,*], Mauro Leoncini [b]

[a] Department of Chemical and Geological Sciences, University of Modena and Reggio Emilia, Modena, Italy
[b] Department of Physics, Informatics and Mathematics, University of Modena and Reggio Emilia, Modena, Italy

HIGHLIGHTS

- Statistical analysis of the data for evaluating the toxicity/carcinogenicity potential of mineral fibres has been performed.
- Distinct classes for amphibole asbestos, chrysotile, erionite, and non-carcinogenic fibres were obtained.
- The rank of potential toxicity/carcinogenicity is amphibole asbestos > erionite > chrysotile.
- Fibrous nano-anatase, nano-goethite, calcite and datolite are classified as non-hazardous.
- Short chrysotile fibres (L≤5μm) fall outside the class of carcinogenic chrysotiles but above the threshold limit for potentially toxic/carcinogenic fibres.

GRAPHICAL ABSTRACT

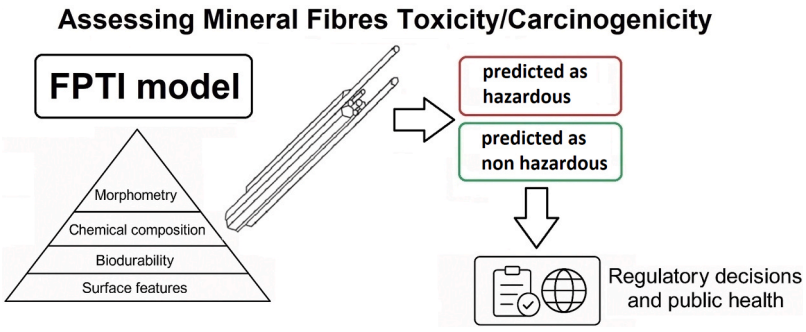

ARTICLE INFO

Keywords:
Mineral fibres
Asbestos
Toxicity
Carcinogenicity
FPTI

ABSTRACT

This work reports the results of a statistical analysis for evaluating the toxicity/carcinogenicity potential of mineral fibres using the Fibre Potential Toxicity Index (FPTI), a quantitative model designed to assess the toxicity and carcinogenicity of mineral fibres based on their physical, chemical, and morphological characteristics. The FPTI model evaluates 18 parameters of mineral fibres, such as morphometry, chemical composition, biodurability, and surface features, which contribute to adverse effects *in vitro* and *in vivo*. The model has been used to evaluate several mineral fibres, namely asbestos minerals and erionite. Recent statistical analysis of these data has led to the creation of representative classes for various fibres, allowing for the evaluation of new fibres with industrial, economic, or social significance. The analysis allowed to draw distinct classes of fibres classified as IARC *Group* 1 carcinogenic agents (amphibole asbestos, erionite, and chrysotile) and fibres classified as IARC *Group 3* agents (sepiolite and wollastonite). The study identifies fibre size, metals' content, and dissolution rate as critical parameters of the model. The FPTI model serves as a preliminary screening tool, complementing other predictive models, to inform regulatory decisions and IARC classification processes for mineral fibres that may pose risks to public health.

* Correspondence to: Department of Chemical and Geological Sciences, University of Modena and Reggio Emilia, Via G. Campi 103, Modena 41125, Italy.
E-mail address: alessandro.gualtieri@unimore.it (A.F. Gualtieri).

https://doi.org/10.1016/j.jhazmat.2025.139202
Received 28 April 2025; Received in revised form 2 July 2025; Accepted 8 July 2025
Available online 9 July 2025

1. Introduction

Today, one of the top missions of health and environmental institutions worldwide is the identification, evaluation and quantification of the risks associated to natural and man-made toxic/carcinogenic agents to develop management plans aimed at minimising the risk of exposure for the general public and workers. At a national level this task is entrusted to government organizations such as the Environmental Protection Agency (EPA) in the USA and the "Istituto Superiore di Sanità" (ISS) in Italy. At a global level, the International Agency for Research on Cancer (IARC), under the umbrella of the World Health Organization (WHO), is certainly the major player. Every year, IARC delivers Monographs from expert Working Group for the evaluation/re-evaluation of carcinogenic hazards to humans [2]. Such evaluations have regarded several mineral fibres in the past, with a special attention to asbestos, erionite and asbestos-like minerals (*e.g.* fluoro-edenite). For the evaluation of carcinogens, tools suitable for toxicity prediction (prediction toxicology) are promoted today, combining innovative data-mining and in silico methods, trying as much as possible to limit *in vivo* testing. A remarkable example is the *ToxCast* research program of the Environmental Protection Agency (EPA) to predict the potential toxicity of environmental chemicals based on *in vitro* bioactivity profiling [21].

In this scenario, a project to develop a quantitative predictive model of toxicity/carcinogenicity of minerals fibres based on the physical-chemical and morphological parameters started ten years ago. The Fibre Potential Toxicity Index (FPTI) model delivers an index for mineral fibres to classify their potential toxicity and carcinogenicity [28,34]. For the determination of the FPTI index, the model evaluates the morphometric, chemical, biodurability-related, and surface parameters of mineral fibres responsible for adverse effects *in vitro* and *in vivo* [27]. The size (length and width) of mineral fibres is a key factor influencing their toxicity, inflammatory response, and pathogenicity [17]. Additionally, fibre surface curvature plays a crucial role in protein binding and cell adhesion [11]. The shape of a fibre determines its deposition pathway in the respiratory tract while its density affects its aerodynamic diameter, which in turn influences the depth of fibre deposition within the airways [36]. The hydrophobicity of a fibre regulates its interaction with biopolymers and phagocytes. Surface area impacts dissolution kinetics and biodurability, which dictate resistance to chemical and biochemical alteration [36]. Iron and other metals like Ni, Mn, V are key toxicity chemical factor. Iron present on the fibre surface facilitates the formation of reactive oxygen species (ROS), leading to cyto- and genotoxic effects [50]. The dissolution rate of a fibre is a cornerstone of the fibre toxicity paradigm [17]. If a fibre rapidly dissolves in lung fluids - indicating low biodurability - it is generally considered less toxic due to lower biopersistence [36]. The dissolution rates of iron, silica, and other metals regulate the extracellular release of substances that can generate ROS [35]. Additionally, the electric charge of the fibres, measured as zeta potential, is associated with various adverse biological effects, including hemolysis, cross-talk phenomena, and apoptosis. The zeta potential also influences the agglomeration of the fibre in the lung fluids [56]. *In vivo*, some silicates like fibrous zeolites may exchange cations, potentially disrupting cellular life cycles [3,60]. A detailed description of each parameter of the model is found in Gualtieri et al. [36] and Gualtieri [26]. A value is assigned to each of the 18 parameters, depending on its susceptibility to prompt adverse effects and subsequent inclusion in one of the value classes T_i. Because the parameters of the model can correlate with each other, a hierarchical scheme that considers cross-correlations is also applied [26]. The code which defines the hierarchy of the parameter is H and the weight applied with respect to H is defined as $W_1 = 1/H$, with H = 1, 2 or 3. From Table 1, showing all the parameters of the model, first rank parameters (H=1) are: (1,1) mean fibre length, (1,2) mean fibre width, (1,3) crystal curvature, (1,4) crystal habit, (1,8) total iron content, (1,11) content of metals other than iron, (1,16) zeta potential, and (1,18) cation exchange. Second rank

Table 1
The parameters of the FPTI model.

Parameter	H	U	Classes	Normalized score $FPTI_i$
(1,1) mean fibre length L (μm)	1	1	$L \leq 5.0$	0.0
			$5.0 < L \leq 10.0$	0.1
			$10.0 < L \leq 20.0$	0.2
			$L > 20.0$	0.4
(1,2) mean fibre width D (μm)	1	1	$D > 3.0$	0.0
			$1.0 < D \leq 3.0$	0.1
			$0.25 < D \leq 1.0$	0.2
			$D \leq 0.25$	0.4
(1,3) crystal curvature	1	2	lat surface	0.05
			altered surface	0.1
			cylindrical surface	0.2
(1,4) crystal habit	1	1	Curled	0.1
			mixed Curled/acicular	0.2
			acicular	0.4
(1,5) fibre density ρ (g/cm^3)	2	1	$\rho \leq 2.75$	0.05
			$2.75 < \rho \leq 3.5$	0.1
			$\rho > 3.5$	0.2
(1,6) hydrophobic character of the surface	2	1	hydrophobic	0.05
			amphiphilic	0.1
			hydrophilic	0.2
(1,7) specific surface area SSA (m^2/g)	2	1	$SSA > 25.0$	0.05
			$5.0 < SSA \leq 25.0$	0.1
			$0 < SSA \leq 5.0$	0.2
(1,8) total iron content Fe_2O_3+FeO (wt%)	1	2	$Fe_2O_3+FeO = 0.0$	0.0
			$0 < Fe_2O_3+FeO \leq 1$	0.05
			$1 < Fe_2O_3+FeO \leq 10$	0.1
			$Fe_2O_3+FeO > 10$	0.2
(1,9) ferrous iron FeO (wt%)	2	1	$FeO = 0.0$	0.0
			$0.0 < FeO \leq 0.25$	0.05
			$0.25 < FeO \leq 1.0$	0.1
			$FeO > 1.0$	0.2
(1,10) nuclearity or iron atoms n	3	2	$n = 0$	0.0
			$n > 2$	0.02
			$n = 2$	0.03
			$n = 1$	0.07
(1,11) content of metals other than iron* (ppm/ppm)	1	1	$\sum_i \frac{C_i}{L_i} = 0.0$	0.0
			$0.0 < \sum_i \frac{C_i}{L_i} \leq 1.0$	0.1
			$1.0 < \sum_i \frac{C_i}{L_i} \leq 5.0$	0.2
			$\sum_i \frac{C_i}{L_i} > 5.0$	0.3
(1,12) fibre dissolution time t** (y)	2	1	$t \leq 1.0$	0.05
			$1 < t \leq 40.0$	0.1
			$t > 40.0$	0.2
(1,13) velocity of iron release v_R*** (wt%/y)	3	1	$v_R = 0.0$	0.0
			$0.0 < v_R \leq 0.1$	0.03
			$0.1 < v_R \leq 1$	0.07
			$v_R > 1$	0.13
(1,14) velocity of silica dissolution v_S**** (wt %/y)	3	2	$v_S = 0.0$	0.0
			$0.0 < v_S \leq 0.5$	0.02
			$0.5 < v_S \leq 1.0$	0.03
			$v_S > 1.0$	0.07
(1,15) velocity of release of metals v_M***** (ppm/y)	3	1	$v_M = 0.0$	0.0
			$0.0 < v_M \leq 1.0$	0.03
			$1.0 < v_M \leq 10.0$	0.07
			$v_M > 10.0$	0.13
(1,16) zeta potential ζ (mV)	1	2	(-) at pH= 4.0–4.5	0.1
			(-) at both pH= 4.0–4.5 and 7.0–7.4	0.2
(1,17) ζ values[N] inducing fibres' aggregation (mV)	3	1	$\zeta > 20.0$ or $\zeta < -20.0$	0.03
			$10.0 < \zeta \leq 20.0$ or $-20.0 \leq \zeta < -10.0$	0.07
			$0.0 \leq \zeta \leq 10.0$ or $-10.0 \leq \zeta \leq 0.0$	0.13
(1,18) cation exchange	1	3	cation exchange	0.07
			no cation exchange	0

[N] at the pH= 7.4 of the extracellular environment.

* $\sum_i \frac{C_i}{L_i}$=sum of the concentrations of metals (Sb, As, Hg, Cd, Co, Cr, Cu, Pb, Ni, Zn, V, Be) C_i in the fibre (ppm) divided by the limit L_i for that metal according to the existing regulatory system [68] except for Be with limit = 0.5 ppm;

** the total dissolution time of the fibre calculated in years (y) following the standardized acellular *in vitro* dissolution model at pH= 4.5 described in Gualtieri et al. [37];

*** total content of elemental iron in the fibre (wt%) possibly made available as active iron at the surface of the fibre divided by the total dissolution time (y) of the fibre (y);

**** total content of Si of the fibre (wt%) divided by the total dissolution time (y) of the fibre;

***** total content (ppm) of heavy metals (Sb, As, Hg, Cd, Co, Cr, Cu, Pb, Ni, Zn, V, Be, Mn) divided by the total dissolution time (y) of the fibre;

Table 2
The mineral fibres considered in this study for the statistical analysis of the data delivered by the FPTI model.

fibre	origin	L(μm), W(μm) *	$FPTI_i$ (error**)	reference ***
amosite UICC	Penge, Northern Province (South Africa) NB #4173–111–4	66.0, 0.1	3.17 (0.13)	[57]
asbestos actinolite	San Severino, Basilicata (Italy)	50.0, 0.2	3.03 (0.20)	[7]
asbestos anthophyllite UICC	Paakkila (Finland) NB #4173–111–5	25.0, 0.4	2.77 (0.17)	[57]
asbestos tremolite	Lanzo Valley, Piedmont (Italy)	45.0, 1.1	2.88 (0.13)	[51]
chrysotile	Balangero, Torino (Italy)	35.0, 1.5	2.35 (0.08)	[20]
chrysotile UICC	"B" Canadian NB #: 4173–111–1	52.0, 0.27	2.22 (0.07)	[58]
chrysotile	Valmalenco, Sondrio (Italy)	8.1, 0.07	2.25 (0.26)	[8]
chrysotile	Yasniy, Orenburg Oblast (Russia)	33.9, 0.07	2.40 (0.07)	[15]
crocidolite UICC	Koegas, Northern Cape of South Africa NB #: 4173–111–3	25.0, 0.3	2.73 (0.08)	[52]
erionite	Gawler Downs, Canterbury (New Zealand)	210.0, 0.39	2.43 (0.04)	[55]
erionite	Jersey, Nevada (USA)	9.39, 0.24	2.28 (0.21)	[30]
erionite	Karain, Cappadocia, Turkey	12.5, 0.5	2.33 (0.07)	[16]
erionite	Kaipara, North Island (New Zealand)	16.0, 0.7	2.33 (0.03)	[62]
erionite	Tuzköy, Cappadocia, Turkey	24.5, 0.81	2.48 (0.05)	[24]
fibrous fluoro-edenite	Biancavilla, Catania (Italy)	100.0, 0.5	2.60 (0.11)	[25]
fibrous sepiolite	Vallecas, Madrid (Spain)	7.0, 0.15	1.68 (0.08)	[67]
fibrous wollastonite NYAD G−1	Essex County, New York (USA)	11.0, 1.1	1.92 (0.14)	[14]
fibrous wollastonite NYAD G−2	Essex County, New York (USA)	46.6, 2.99	2.08 (0.11)	[14]

* mean value of the fibre length and width;

** calculated with the new version of webFPTI available online at the link: https://fibers-fpti.unimore.it/FPTI/. The manual (WebFPTI_Manual_version4c_250205) reports the scheme for the calculation of the errors for each parameter of the model;

*** reference for the description and characterization of the sample.

parameters (H=2) are: (1,5) fibre density, (1,6) hydrophobic character of the surface, (1,7) specific surface area, (1,9) ferrous iron, and (1,12) fibre dissolution time. Third rank parameters (H=3) are: (1,10) nuclearity or iron, (1,13) velocity of iron release, (1,14) velocity of silica dissolution, (1,15) velocity of release of metals, (1,17), and fibres' aggregation. For example, H= 2 (hierarchy=2) is assigned to the specific surface area (1,7) because it depends upon the length (H=1) and diameter (H=1) of the fibre. H= 3 (hierarchy=3) is assigned to the velocity of release of metals (1,13) because this parameter depends upon a first rank parameter (H=1) like the content of metals other than iron (1, 11) and a second rank parameter (H=2) like the specific surface area (1, 7). The complete scheme of the hierarchical clustering in the FPTI model is published as Fig. 1 in Gualtieri [26] and Mossman and Gualtieri [49].

A second weight defined as w_2= 1/U is also applied to each parameter. It accounts for the uncertainty in the determination of a specific parameter and is defined by the penalty parameter U (1 = low to null uncertainty, 2 = some degree of uncertainty, 3 = high uncertainty). Specifically, it refers to the level of knowledge to which a model parameter causes adverse bio-chemical effects *in vitro/in vivo* obtained from literature data. The more literature data exist on the correlation of that parameter with one or more adverse effects, the lower the value (penalty parameter U=1=low to null uncertainty). Few ambiguous literature data result in a penalty parameter U= 3 (high uncertainty). For example, U= 1 is assigned to the parameter (1,1) mean fibre length because it is well known that it prompts, among others effects, indirect production of electrophilic species like hydroxyl radicals (ROS) and genotoxic ROS/RNS (reactive nitrogen species) during AM frustrated phagocytosis [27]. On the other hand, U= 3 is assigned to the parameter (1,18) cation exchange because only few recent evidences suggest its role in inducing adverse effects *in vitro* (see the case of erionite in [3]).

The FPTI score of each fibre is the sum of all individual $FPTI_i$ values, classified and weighed according to the equation [26]:

$$FPTI = \sum_{i=1}^{n} W_1 W_2 T_i$$

with W_1= 1/H, weight of the parameter according to its hierarchy H; W_2= 1/U, weight of the parameter according to the uncertainty U of its evaluation (see above); T_i=class value of the parameter i of the model. As anticipated above, Table 1 reports all the parameters of the model, with the hierarchy factor H, the uncertainty factor U, the classes and normalized $FPTI_i$ scores.

Gualtieri et al. [31] have recently shown how the 18 FPTI parameters of the mineral fibres that induce specific adverse effects are tied to *in vivo* pathological processes attributed to the characteristics of carcinogens KCs used by IARC to evaluate an agent. Specifically, these KCs are KC1: Is electrophilic or can be metabolically activated to electrophiles? KC2: Is genotoxic? KC3: Alters DNA repair and causes genomic instability? KC4: Induces epigenetic alterations? KC5: Induces oxidative stress? KC6: Induces chronic inflammation? KC7: Is immunosuppressive? KC8: Modulates receptor-mediated effects? KC9: Causes immortalization? KC10: Alters cell proliferation, cell death or nutrient supply? [39,64]. It is remarked that Table 3 in Gualtieri [27] summarizes the 18 FPTI parameters and their role in contributing to the 10 KCs.

Although the FPTI model stands on the shoulders of solid existing models such as the Toxicity Estimation Software Tool (T.E.S.T.) for the estimation of the toxicity from molecular structure developed by the U.S. Environmental Protection Agency EPA [69], its novelty lies in the fact it has been especially developed to study fibrous particles and predict their toxicity/carcinogenicity from all the physical-chemical-crystallographic properties. FPTI distinguishes from solid existing tools such as *ToxCast* which predicts the potential toxicity of chemicals based just on *in vitro* testing data [21] or QSAR, a quantitative structure–activity relationship generalist model [54] which predicts how the chemical structure of molecules (not complex natural phases like mineral fibres) affects their biological (adverse) activities or physico-chemical properties.

The FPTI model is implemented in WebFPTI, a web-based application structured as a classical three-tier architecture. WebFPTI has been developed and runs under a Debian GNU Linux OS [34]. The software is available online at the link: https://fibers-fpti.unimore.it/FPTI/. The manual is also available as *pdf* file (WebFPTI_Manual_version4c_250205

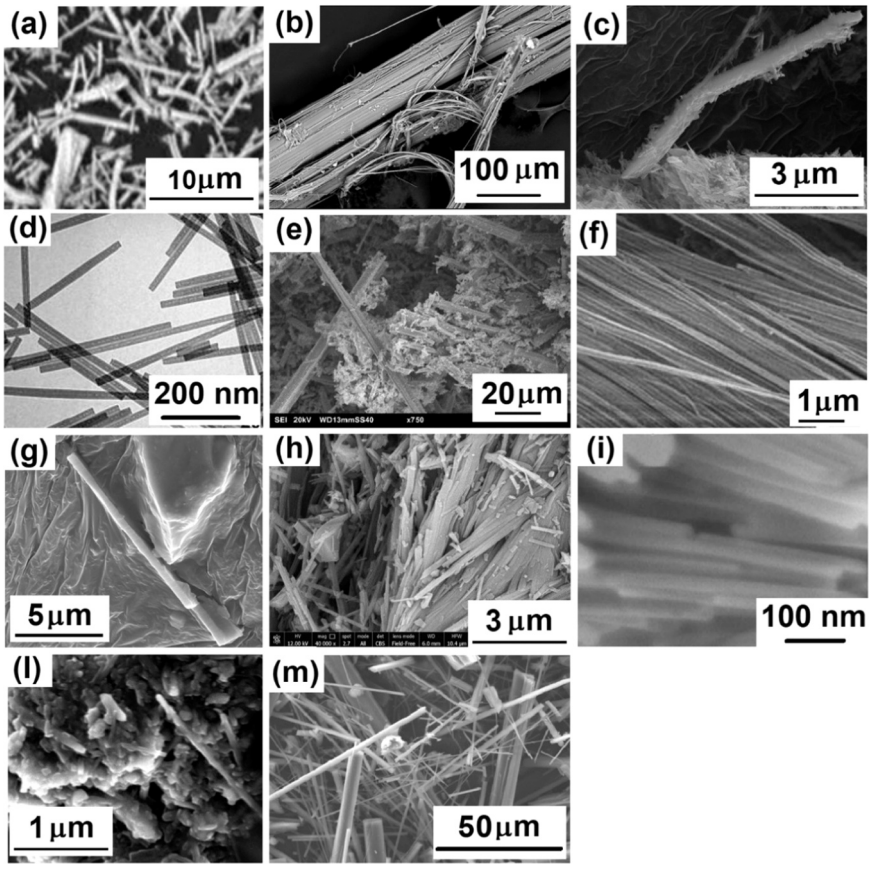

Fig. 1. SEM images of the fibres were evaluated in this work: (a) synthetic commercial anatase nano-fibres (914401, Sigma-Aldrich) (modified from www.sigmaaldrich.com/IT/it/product/aldrich/914401); (b) commercial natural chrysotile from Yasniy, Orenburg Oblast (Russia), with mean fibre length L> 5μm; (c) commercial natural chrysotile from Yasniy, Orenburg Oblast (Russia), with mean fibre length L≤ 5μm; (d) synthetic iron-free nano-chrysotile; (e) fibrous boulangerite from Trepča Stari Trg, Mitrovica District Kosovo; (f) a synthetic fibrous calcite; (g) natural fibrous datolite from Berceto, Parma (Italy); (h) fibrous glaucophane from San Anselmo, Marin County, California (USA) [13]; (i) synthetic goethite nano-fibres; (l) commercial natural halloysite nano-tubes from Matauri Bay, Northern Island (New Zealand); (m) mordenite from Poona (India).
(f) (modified from [40]); (h) (modified from [38]); (m) (modified from [12]).

at the date of manuscript publication) and reports the scheme for the calculation of the errors for each parameter of the model. Specifically, errors consider how close the value is to the adjacent class limit. For the threshold values, the error is the half of the variation (Δ) between adjacent FPTI scores. The error varies with the distance from the threshold values following an exponential decay:

$(\Delta/2)/e^{s}$

with Δ=half of the variation between adjacent FPTI scores; s = step between the values of the parameters. In the manual, tables are provided to calculate the errors associated to the FTPI score for each fibre parameter in the parameter interval of values. Let us consider an example relative to the fibre length L parameter. If the measured value of the mean fibre length Lis 10 μm, the error associated to the FPTI score of the fibre length L parameter is 0.05. This number is half of the difference values between the class of FPTI 0.1 and 0.2 (0.2–0.1 =0.1; 0.1/2 =0.05). Error decreases following the exponential decay above with the distance from the threshold value (10 μm). If the measured value of the mean fibre length L= 13 μm, the error associated to the FPTI score of the fibre length L parameter is 0.002489, that is $[(0.05)/2]/e^{(13-10)}$. The qualitative parameters (1,3), (1,4), (1,6), (1,16), and (1,18) (Table 1) have an associated Error= 0.

In the last ten years, the FPTI model has been used to evaluate several mineral fibres (e.g. asbestos: [26]; fibrous glaucophane: [13]; erionite: [55]; chrysotile: [15]), wollastonite: [14]).

In this work, a statistical analysis of the data collected so far was conducted to create representative classes of values for amphibole asbestos, chrysotile, erionite, and fibres that belong to IARC *Group 3* (evaluated as "not classifiable as to their carcinogenicity to humans due to inadequate evidence of carcinogenicity in humans and animals"). These classes of values are used for the *ab initio* evaluation of mineral fibres of industrial, economic or social importance such as anatase nano-fibres, chrysotile from Russia, nano-chrysotile [41], fibrous boulangerite from Kosovo, fibrous calcite [40], fibrous datolite from Italy, synthetic goethite nano-fibres [38], halloysite nano-tubes from New Zealand. Fibrous glaucophane from California (USA) and mordenite from India have already been characterized and evaluated by Di Giuseppe et al. [13] and Di Giuseppe [12] but have been included here to refine the general model.

2. Materials and methods

The mineral fibres investigated elsewhere and used in this study for the statistical analysis of the FPTI data are reported in Table 2. For each mineral fibre, the table reports the origin of the sample, the mean values of the fibre length L (μm) and width W (μm), the FPTI score with associated error, and the reference describing the sample characteristics. The evaluated amphiboles are: standard UICC amosite from Penge, Northern Province (South Africa) NB #4173–111–4; asbestos actinolite from San Severino, Basilicata (Italy); standard UICC asbestos anthophyllite from Paakkila (Finland) NB #4173–111–5; UICC standard crocidolite from Koegas, Northern Cape of South Africa NB #: 4173–111–3; asbestos

Table 3
The unclassified/unregulated mineral fibres evaluated in this study with the FPTI model.

fibre	origin	L(μm), W(μm)*	$FPTI_i$ (error**)	reference ***
anatase nano-fibre	synthetic commercial 914401 from Sigma-Aldrich	6.0, 0.5	1.43 (0.03)	www.sigmaaldrich.com
chrysotile L> 5μm	Yasniy, Orenburg Oblast (Russia)	29.8, 0.4	2.35 (0.05)	[63]
chrysotile L≤ 5μm	Yasniy, Orenburg Oblast (Russia)	1.91, 0.15	2.18 (0.07)	[63]
nano-chrysotile	synthetic	1.0, 0.05	1.37 (0.02)	[41]
fibrous boulangerite	Trepča Stari Trg, Mitrovica District Kosovo	23.0, 2.5	2.50 (0.04)	[19]
fibrous calcite	synthetic	15.0, 0.10	1.68 (0.03)	[40]
fibrous datolite	Berceto, Parma, Italy	9.68, 1.38	1.50 (0.10)	[74]
fibrous glaucophane	San Anselmo, Marin County, California, USA	4.0, 0.22	2.77 (0.04)	[13]
goethite nano-fibres	synthetic, sample 25	0.47, 0.07	1.73 (0.04)	[38]
halloysite nano-tubules	Matauri Bay, Northern Island, New Zealand	1.5, 0.13	1.92 (0.10)	[33]
mordenite	Poona (India)	20.8, 0.95	2.02 (0.14)	[12]

* mean value of the fibre length and width;
** calculated with the new version of webFPTI available online at the link: https://fibers-fpti.unimore.it/FPTI/. The manual (WebFPTI_Manual_version4c_250205) reports the scheme for the calculation of the errors for each parameter of the model;
*** reference for the description and characterization of the sample.

tremolite from Lanzo Valley, Piedmont (Italy). Evaluated chrysotiles are from Balangero, Torino (Italy); UICC standard "B" Canadian NB #: 4173–111–1; Valmalenco, Sondrio (Italy); Yasniy, Orenburg Oblast (Russia). Evaluated erionites are from Gawler Dows, Canterbury (New Zealand); Jersey, Nevada (USA); Karain, Cappadocia, Turkey; Kaipara, North Island (New Zealand); Tuzköy, Cappadocia, Turkey. Fibrous fluoro-edenite from Biancavilla, Catania (Italy), fibrous sepiolite from Vallecas, Madrid (Spain) and two commercial samples of fibrous wollastonite NYAD G from Essex County, New York (USA) were also analysed.

In this work, the following mineral fibres were also evaluated: synthetic commercial anatase (TiO_2) nano-fibres (914401, Sigma-Aldrich); commercial natural chrysotile from Yasniy, Orenburg Oblast (Russia) $[(Mg_{2.870}Fe^{2+}_{0.027}Fe^{3+}_{0.044}Al_{0.034}Cr_{0.005}Ni_{0.006})(OH)_4Si_{1.982}O_5]$, with mean fibre length L> 5μm; commercial natural chrysotile from Yasniy, Orenburg Oblast (Russia), with mean fibre length L≤ 5μm. Two size classes of the natural commercial sample were obtained by cryogenic milling. The batch of the short (≤5μm) chrysotile fibres has a mean fibre length of 1.91μm, a mean fibre width of 0.15μm and a specific surface specific area of 30 m^2/g while the batch of the long (>5μm) chrysotile fibres has a mean fibre length of 29.8μm, a mean fibre width of 0.4μm and a specific surface specific area of 28.9 m^2/g. [63]; synthetic iron-free nano-chrysotile ($Mg_3(OH)_4Si_2O_5$) [41]; fibrous boulangerite ($Pb_5Sb_4S_{11}$) Trepča Stari Trg, Mitrovica District (Kosovo); a synthetic fibrous calcite ($CaCO_3$) [40]; natural fibrous datolite [$CaB(SiO_4)(OH)$] from Berceto, Parma (Italy); fibrous glaucophane from San Anselmo, Marin County, California (USA) $(K_{0.01}(Na_{1.61}Ca_{0.43})(Mg_{2.01}Fe^{+2}_{1.31}Fe^{+3}_{0.70}Al_{1.00}Mn_{0.06})Si_{8.09}O_{22}(OH)_2)$, fully characterized in [13]); synthetic goethite (FeOOH) nano-fibres described in Kosmulski et al. [38]; commercial natural halloysite $[Al_2(OH)_4Si_2O_5{\cdot}2\ H_2O]$ nano-tubes from Matauri Bay, Northern Island (New Zealand); zeolite mordenite from Poona (India) $[(Na_{3.63}K_{0.16}Ca_{1.87}Mg_{0.07})[Al_{7.21}Si_{40.67}O_{96}]{\cdot}28\ H_2O]$, fully characterized in Di Giuseppe [12].

Fig. 1 reports a gallery of the fibres evaluated in this work. Specifically: (a) synthetic anatase nano-fibres; (b) Russian chrysotile with mean fibre length L> 5μm; (c) Russian chrysotile with mean fibre length L≤ 5μm; (d) synthetic nano-chrysotile; (e) fibrous boulangerite from Kosovo; (f) synthetic fibrous calcite; (g) fibrous datolite from Italy; (h) fibrous glaucophane from USA; (i) synthetic goethite nano-fibres; (l) commercial halloysite nano-tubes from New Zealand; (m) mordenite from India.

This section describes the way the 18 parameters of the FPTI model (Table 1) were calculated. For the morphometric parameters (1,1) mean fibre length L, (1,2) mean fibre width D, (1,3) crystal curvature, and (1,4) crystal habit, experimental scanning electron microscopy (SEM) (see the gallery in Fig. 1) or transmission electron microscopy (TEM) data were collected (following the experimental protocol applied in [37]), except for synthetic anatase nano-fibres, synthetic fibrous calcite, and synthetic goethite nano-fibres whose data were taken from the available literature data (see the references reported in Table 3). The ideal fibre density [parameter (1,5)] of the fibres was taken from the mineralogical database webmineral.com. The hydrophobic character of the surface [parameter (1,6)] was evaluated from experimental zeta potential values [parameter (1,16)], following the experimental protocol applied in Pollastri et al. [56], or from the literature data. The specific surface area SSA [parameter (1,7)] was measured experimentally, using the Brunauer-Emmett-Teller (BET) method (used for example in Gualtieri et al. [37]) or calculated geometrically from the size parameters of the fibre in the case of synthetic anatase nano-fibres, fibrous boulangerite from Kosovo, synthetic fibrous calcite, and synthetic goethite nano-fibres. Regarding the iron-related parameters (1,8) total iron content, (1,9) ferrous iron, and (1,10) nuclearity or iron atoms, they were experimentally measured and calculated using the model described in Gualtieri et al. [31] for the Russian chrysotiles, fibrous glaucophane, and the commercial halloysite nano-tubes. Synthetic anatase, synthetic nano-chrysotile, fibrous boulangerite, synthetic fibrous calcite, fibrous datolite, and mordenite are assumed to be iron-free. Synthetic goethite nano-fibres are assumed to have ideal FeOOH chemical formula with cluster iron nuclearity [31]. The content of metals [parameter (1,11)] other than iron was measured experimentally using electron probe microanalysis (EPMA) (see an example of the application of the methodology in [37]) for the Russian chrysotiles, synthetic nano-chrysotile, fibrous boulangerite, fibrous datolite, fibrous glaucophane, halloysite nano-tubes, and mordenite. Synthetic anatase nano-fibres, synthetic fibrous calcite, and synthetic goethite nano-fibres are assumed to be free of metals.

Fibre dissolution times [parameter (1,12)] were experimentally determined (see the procedure in [37]) for the chrysotile species and for fibrous glaucophane [13] and mordenite [12]. Dissolution times of the other fibres were calculated starting from the sample size, chemical data and literature data: Mbanga et al. [44] for anatase; Achimovičová, Baláž [1] for boulangerite; Cornell et al. [9] for goethite. Dissolution of calcite in acidic medium is assumed to be instantaneous. For datolite, there are no dissolution rates available in the literature. Hence, dissolution data of danburite was considered [73]. For halloysite, kaolinite $[Al_2(OH)_4Si_2O_5]$ dissolution rates were used as input data [72].

The "release" parameters [(1,13) velocity of iron release, (1,14) velocity of silica dissolution, and (1,15) velocity of release of metals] are calculated from the previous parameters (1,8), (1,11) and (1,12) while the content of Si is determined from the measured chemical composition of the sample determined using EPMA (again, see an example of the application of the methodology in [37]). The values of zeta potential-related parameters (1,16) and (1,17) were measured experimentally (see above) for the Russian chrysotiles, fibrous datolite, fibrous glaucophane, halloysite nano-tubes, and mordenite. Data were taken from the literature for synthetic anatase nano-fibres, synthetic nano-chrysotile, fibrous boulangerite, synthetic fibrous calcite, and synthetic goethite nano-fibres. The last parameter (1,18), ability to

exchange cations in suspension, only applies here to zeolite phases. This chemical property is not measured as the (1,18) parameter is only qualitative (yes=capability of cation exchange; no=inability of cation exchange).

3. Results

All the 18 parameters used to calculate the FPTI score for each analysed fibre are available online in the WebFPTI application environment at the link https://fibers-fpti.unimore.it/FPTI/materials/).

Fig. 2 and Table 2 report the FPTI score, and relative error, for the evaluated mineral fibres. The histogram plot evidences the differences of the various groups of amphibole asbestos fibres (in black), erionite fibres (in dark grey), chrysotile fibres (in light grey), and the fibres assumed to be non-hazardous or unclassified (in white).

Fig. 3 and Table 3 report the mean FPTI score with standard deviation of the different groups of mineral fibres. Amphibole asbestos (black) with a mean FPTI score of 2.86 (0.21), erionite (dark grey) with a mean FPTI score of 2.37 (0.08), and chrysotile (light grey) with a mean FPTI score of 2.30 (0.09), are classified as IARC *Group* 1 carcinogenic agents. Sepiolite and wollastonite are classified as IARC *Group 3* agents (white) with a mean FPTI score of 1.89 (0.20). Fibrous nano-anatase, nano-goethite, calcite and datolite are IARC non-classified agents (white) and assumed to be non-hazardous. Their mean FPTI score is 1.59 (0.59). The mean values considered eventual outliers calculated using the Interquartile Range (IQR) method [48].

A statistical analysis was performed with the Kruskal-Wallis test using the application available online at http://www.statskingdom.com/kruskal-wallis-calculator.html. The results of the tests are provided as Supplementary Material 1. The Kruskal-Wallis H test indicated that there is a significant difference in the dependent variable between the different groups, $\chi^2(3) = 14.46$, $p = 0.002$, with a mean rank score of 15.5 for Group1 (amphibole asbestos), 8.8 for Group2 (erionite), 7 for Group3 (chrysotile), 2 for Group4 (IARC *Group 3* fibres). The Post-Hoc Dunn's test using a Bonferroni corrected alpha of 0.0083 indicated that the mean rank of the x_1-x_4 pair is significantly different.

Fig. 4 depicts a comparative plot of the mean FPTI score as square dots with standard deviation of the different groups of mineral fibres.

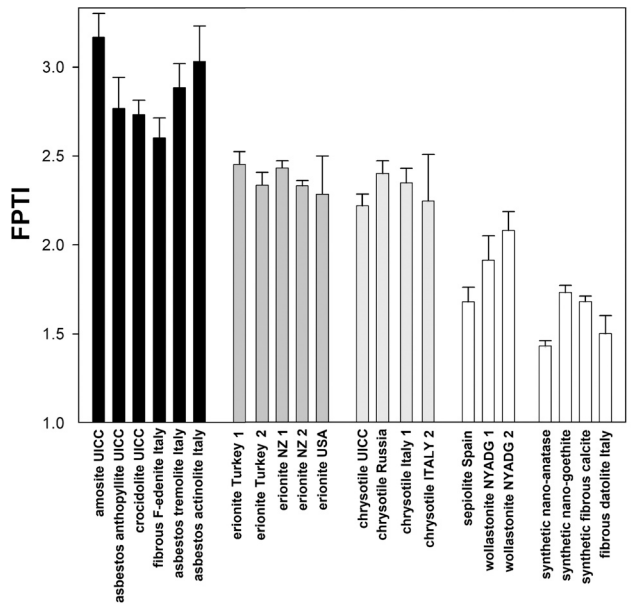

Fig. 2. Histogram plot depicting the FPTI score (with relative error) of different mineral fibres. Legend: group of amphibole asbestos fibres = black; group of erionites = dark grey; group of serpentine asbestos, chrysotile = light grey; fibres assumed to be non-hazardous or that are unclassified fibres = white.

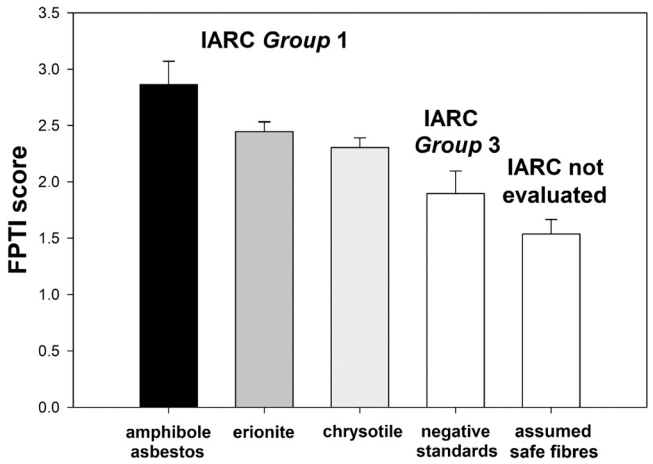

Fig. 3. Histogram comparative plot of the mean FPTI score (with standard deviation) of the different groups of mineral fibres. Legend: fibres classified as IARC *Group* 1 carcinogenic agents (amphibole asbestos = black; erionite = dark grey; chrysotile = light grey); Fibres classified as IARC *Group 3* agents (sepiolite and wollastonite are =white). Fibres that are IARC non-classified agents or assumed to be non-hazardous (fibrous nano-anatase, nano-goethite, calcite and datolite) = white.

The limits of the areas relative to each group are the calculated standard deviations. The right side of the plot reports the FPTI score as square dots, with standard deviation, of unclassified fibres evaluated in this work. Specifically, from the higher score to the lower score: fibrous glaucophane, fibrous boulangerite, Russian chrysotile, synthetic nano-chrysotile, mordenite and halloysite nano-tubes.

4. Discussion

After 10 years of work aimed at the classification of the potential toxicity/carcinogenicity of mineral fibres using the FPTI model, the collected data allowed us to attempt a statistical analysis and generate representative classes of values for amphibole asbestos, chrysotile, erionite, and IARC *Group 3* fibres. These classes can be used for the *ab initio* evaluation of other unclassified mineral fibres of industrial, economic or social importance.

It should be remarked that the FPTI *ab initio* model is conceptually a basic comparative tool to predict the toxicity/pathogenicity potential of a respirable mineral fibre. It relies on a robust dataset of 18 measured or calculated fibre-related parameters that induce bio-chemical mechanisms responsible for cancer-related adverse effects *in vivo* [27]. It is a comparative tool because the obtained FPTI scores are compared to those of positive standards (the mineral fibres classified as carcinogenic to humans according to the IARC) and the negative standards (the mineral fibres not classified as to their carcinogenicity to humans according to the IARC) [32].

4.1. Classified fibres

4.1.1. Comparison of the amphibole asbestos, chrysotile and erionite families

There is a statistically significant different mean FPTI score among the IARC *Group* 1 carcinogenic agents (Fig. 3) with the following rank of potential toxicity/carcinogenicity: amphibole asbestos > erionite > chrysotile. The mean value of the IARC *Group* 1 carcinogenic agent chrysotile of lowest potential [2.30 (0.09)] is well above the mean FPTI score of 1.89 (0.20) displayed by sepiolite and wollastonite samples, classified as IARC *Group 3* agents (white in Fig. 3) and much greater than that [1.59 (0.59)] of non-classified agents fibrous nano-anatase, nano-goethite, calcite and datolite (also white in Fig. 3) assumed to be non-hazardous.

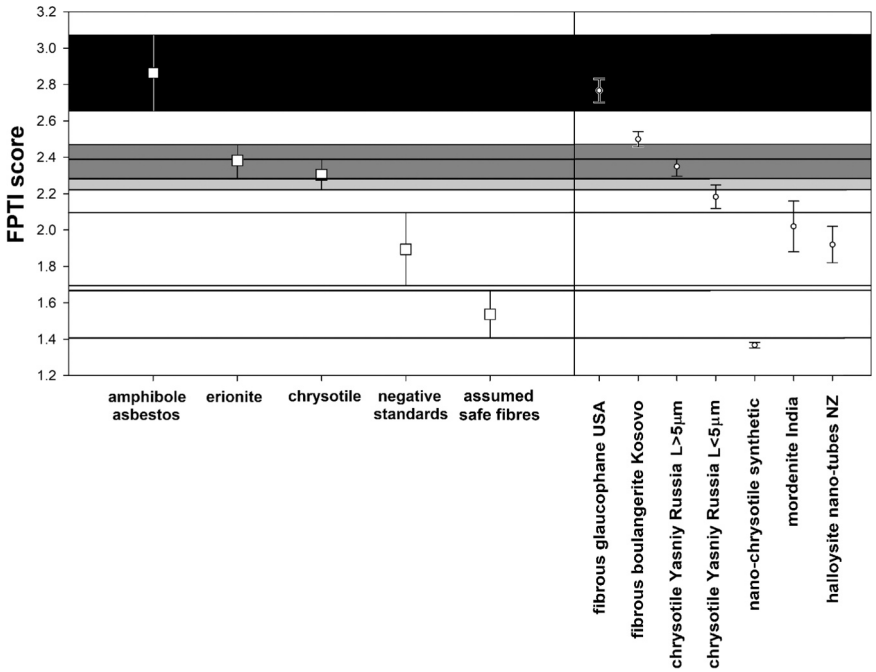

Fig. 4. Comparative plot of the mean FPTI score as square dots, with standard deviation, of the different groups of mineral fibres and relative extended area of each group. On the left side of the plot, amphibole asbestos (black), erionite (dark grey), and chrysotile (light grey) are classified as IARC *Group* 1 carcinogenic agents. Sepiolite and wollastonite are classified as IARC *Group 3* agents, negative standards (white). Fibrous nano-anatase, nano-goethite, calcite and datolite are IARC non-classified agents (white) and assumed to be safe fibres. The right side of the plot reports the FPTI score as square dots, with standard deviation, of unclassified fibres. Specifically, from the higher score to the lower score: fibrous glaucophane, fibrous boulangerite, Russian chrysotile, synthetic nano-chrysotile, mordenite and halloysite nano-tubes.

The rank for the potential toxicity/carcinogenicity (amphibole asbestos > erionite > chrysotile) does not directly compares with the literature data because the latter refer to different tests or data sets (epidemiological data on one or more types of malignancies, *in vivo* tests on animals, *in vitro* tests in various cell cultures). Moreover, these data are often inconclusive and contradictory. Conflicting results may depend on the different cell lines and animal species used in the testing (see Table 1 in [6]).

Regarding epidemiologic data, McDonald and McDonald [45,46] concluded that amphibole fibres are considerably more hazardous than chrysotile in humans. Accordingly, Bernstein and Hoskins [4] reported that chrysotile appears to be less potent for mesothelioma induction than crocidolite. Stayner et al. [65] on the other hand remarked that no conclusive epidemiologic nor toxicologic evidence support the argument that chrysotile is any less potent than other forms of asbestos for inducing lung cancer and Egilman [18], and references therein, recalculated and accounted for clearance of amphibole and found potency ratios to be crocidolite:amosite:chrysotile 26:14:1, in line with other literature data showing a set of potency ratios of 30:15:1.98.

In vivo tests have shown that erionite is apparently highly carcinogenic in both mice [66] and rats [70]. From Sprague-Dawley rats testing, Maltoni et al. [42] showed that erionite is a potent carcinogen more effective than crocidolite and that mesotheliomagenicity decreases in the order amphibole asbestos > chrysotile. Later, Maltoni et al., [43] actually reported that tumour-bearing animals with estimated peritoneal mesothelioma are 97.5 % for crocidolite, 80.0 % for chrysotile and 50.0 % for erionite; for pleural mesothelioma they are 45.0 % for crocidolite, 65.0 % for chrysotile and 87.5 % for erionite.

Regarding *in vitro* data, amphibole asbestos appeared less cytotoxic than chrysotile although both crocidolite and chrysotile were cytotoxic *in vitro* for the mucociliary cell layer of the tracheal mucosa [10]. Poole et al. [59] observed that erionite has qualitatively different activities to those possessed by other mineral fibres and seems quantitatively more active *in vitro* than other pathogenic fibrous dusts. Palekar et al. [53] showed that the adverse effects of erionite were weaker but statistically significant at dose 100 µg/ml with erionite being more reactive than chrysotile and crocidolite. Later, Bertino et al. [5] showed that dose-dependent cytotoxicity occurred in HMC exposed to erionite fibres, although by far lower than that induced by amosite. Conversely, chrysotile-induced cytotoxicity was comparable with that of erionite.

4.1.2. *Fibre parameters that govern the FPTI score*

The analysis of the models of all the analysed mineral fibres indicates that the key fibre parameters that govern the overall FPTI score are the fibre size, content of iron and metals and parameters related to the dissolution rate. Fibre size, content of iron and metals and dissolution rate are the most important parameters contributing to the 10 KCs as suggested by Gualtieri et al. [31]. Metal-free non-biodurable nano-sized fibres virtually display the lowest toxicity/carcinogenicity potential. A striking example is the synthetic iron-free non-biodurable nano-chrysotile synthesized by Lesci et al. [41] with a FPTI score of 1.37 (0.02) (Table 3). Compared to the group of natural chrysotiles with mean value of 2.30 (0.09) (Fig. 2), the decrease of the score is mostly due to the differences in the following parameters: (1,1) mean fibre length L from 0.4 → 0.0 (Δ=-0.4); (1,8) total iron content Fe_2O_3+FeO (wt%) from 0.2 → 0.0 (Δ=-0.2); (1,9) ferrous iron FeO (wt%) from 0.2 → 0.0 (Δ=-0.2); (1,10) nuclearity or iron atoms from 0.07 → 0.0 (Δ=-0.07); (1, 11) content of metals other than iron* from 0.1 → 0.0 (Δ=-0.1).

4.2. *Unclassified mineral fibres*

4.2.1. *Synthetic commercial anatase nano-fibres*

The synthetic commercial anatase (TiO_2) nano-fibres (914401, Sigma-Aldrich) evaluated in this work are extensively used for many industrial applications as absorbent, pigment, filler and many more. Most of the data for the evaluation are taken from the technical data-sheet available online (www.sigmaaldrich.com). The FPTI score of 1.43 (0.03) (Table 3) is one of the lowest calculated values among all mineral

fibres and fully justifies the assumption of minor to null toxicity/carcinogenicity potential of this agent (Fig. 1 and Fig. 2). Parameters that increase the overall FPTI score are the small fibre width W (0.5 μm in Table 3), acicular crystal habit, high fibre density, hydrophilic character, and low absolute values of the zeta potential that favour fibre agglomeration with a high potential biological response. The overall FPTI score is low because of the absence of metals like iron, nickel, chromium that reset the parameters related to their content and release rates.

4.2.2. Natural chrysotile from Yasniy (Russia) with different fibre lengths

This is the commercial sample from Yasniy, Orenburg Oblast (Russia), fully characterized by Di Giuseppe et al. [15]. The sample consists of flexible bundles of long thin fibres. The potential toxicity/carcinogenicity of two classes of chrysotile fibres with mean fibre length L> 5μm (29.8 μm in Table 3) and mean fibre length L≤ 5μm (1.91 μm in Table 3) has been evaluated. Despite the class, all these fibres can penetrate through the respiratory tract and settle in the alveolar space. Notwithstanding, the different fibre length has a major impact on the overall score determining the FPTI score of 2.35 (0.05) for the long fibre chrysotile and 2.18 (0.07) for the short fibre chrysotile (Table 3 and Fig. 4). The long fibre chrysotile is well within the region of the carcinogenic chrysotile fibres while the short fibre chrysotile is outside this region but above the IARC *Group 3* fibres.

In contact with organic solutions reproducing the lysosome fluid at pH= 4.5 and extracellular fluid at pH= 7, respectively, these chrysotile fibres display negative values of zeta potential that may prompt the formation of hydroxyl radicals, apoptosis and binding of collagen and redox-activated Fe-rich proteins [56]. The low absolute values of the zeta potential values favour particle agglomeration [26]. The low values of ferrous iron and total iron [15] decrease the potential although iron, like other metals, is promptly released in the cellular medium because of the fast dissolution rates of the fibres. In fact, the dissolution time of chrysotile asbestos (<1 y) is much shorter than that of biodurable amphibole asbestos species (>50 y) [37].

4.2.3. Fibrous boulangerite from Trepča Stari Trg (Kosovo)

We characterized and evaluated a sample of fibrous boulangerite ($Pb_5Sb_4S_{11}$) from the Trepča Stari Trg, Mitrovica District (Kosovo). This Pb-containing fibre belongs to the family of sulfosalts, minerals that form a genetically well-defined group occurring in specific conditions of ore formation, usually referred to as hydrothermal processes [47]. Boulangerite like other more common sulfosalts (*e.g.* jamesonite $FePb_4Sb_6S_{14}$, robinsonite $Pb_4Sb_6S_{13}$ and zinkenite $Pb_9Sb_{22}S_{42}$) is widespread and often present as secondary mineralization in noble metals (Ag, Au), Pb, Zn, Cu ores. Because boulangerite (and the other fibrous sulfosalts) are not regulated, it is possible that workers in these mining sites, especially when underground, are exposed to these mineral fibres by inhalation of the respirable fraction. The calculated FPTI score of this fibrous boulangerite sample is 2.50 (0.04) (Table 3) and falls in the region between erionite and amphibole carcinogenic fibres, showing the toxicity/carcinogenicity power of this mineral fibre (Fig. 3). The major parameters that make this fibre toxic are the fibre length L (23.0 μm in Table 3), acicular crystal habit, high fibre density, the small calculated specific surface area (0.14 m^2/g), high content of Pb and metals, and the negative values of the zeta potential at pH= 7.4 and 4–4.5. Because this mineral is soluble in acidic medium, the cargo of metals can be promptly released in contact with phago-lysosomes during the phagocytosis act [28].

4.2.4. Synthetic fibrous calcite

The data of the synthetic fibrous calcite ($CaCO_3$) used for the evaluation are taken from Kumar et al. [40]. These fibres were prepared by inorganic/organic thin-film hybrids using a bio-inspired approach. They are unidirectionally oriented on functional poly(N-isopropylacrylamide) (poly(NIPAm)) chosen as the thermo-responsive polymer [40]. The low FPTI score of 1.68 (0.03) (Table 3) justifies the assumption of its minor toxicity/carcinogenicity potential (Fig. 1 and Fig. 2). Toxicity parameters of these fibres are the size (L=15.0 and W=0.1 μm, respectively, in Table 3), acicular crystal habit, hydrophilic character, and low absolute values of the zeta potential that favour fibres' aggregation. The low overall FPTI score is due to the instantaneous dissolution in acidic medium, mimicking the intracellular phago-lysosomes environment during the phagocytosis act of alveolar macrophages, and negligible content of metals which resets the parameters related to their content and rate of release.

4.2.5. Natural fibrous datolite from Berceto, Parma (Italy)

The natural fibrous datolite [$CaB(SiO_4)(OH)$] evaluated here has been collected in Berceto, Parma (Italy). This sample is of scientific importance with no industrial applications so far. The FPTI score of 1.50 (0.1) (Table 3) is one of the lowest calculated values among all mineral fibres and accounts for its null toxicity/carcinogenicity potential (Fig. 1 and Fig. 2). Parameters of datolite increasing the score are the acicular crystal habit, hydrophilic character, the small calculated specific surface area (1.12 m^2/g), and the negative values of the zeta potential at pH= 7.4 and 4–4.5. The low overall FPTI score is due to the absence of metals which cancels the parameters related to their content and release rates.

4.2.6. Fibrous glaucophane from San Anselmo, Marin County, California (USA)

The evaluated sample of natural fibrous glaucophane from San Anselmo, Marin County, California (USA) has been fully characterized elsewhere [13]. Glaucophane is one of the most abundant minerals of blueschist-grade rocks in the Franciscan Complex in California. Glaucophane fibrous habit is common in blueschist-grade rocks and their disturbance by anthropogenic activities may cause dust emissions that expose workers and population. The mean length of the glaucophane fibres is shorter than 5 μm (L=4.0 μm in Table 3) but the aspect ratio is greater than 3:1. Glaucophane is biodurable and has negative values of zeta potential at pH 4.5 [13]. Negative zeta potentials, such as those displayed by glaucophane, may prompt the formation of hydroxyl radicals, affect apoptosis and favour the binding of collagen and redox-activated proteins [56]. Glaucophane fibres have a relatively high ferrous and total iron content. Overall the calculated FPTI of fibrous glaucophane of 2.77 (0.04) (Table 3) falls within the segment of amphibole asbestos species, witnessing its toxicity/carcinogenicity power. The FPTI score of fibrous glaucophane is smaller than that of the other fibrous amphibole species due to the small size of the individual fibres (Table 3) shorter than the threshold limit of 5 μm set for acting successful phagocytosis by alveolar macrophages [28].

4.2.7. Synthetic goethite nano-fibres

The synthetic goethite (FeOOH) nano-fibres evaluated in this work have been prepared and fully characterized by Kosmulski et al. [38]. Goethite nano-fibres are used for different industrial applications as catalysts, bio-fillers, nano-composites and many more. Most of the data used for the evaluation are taken from Kosmulski et al. [38]. The low FPTI score of 1.73 (0.04) (Table 3) explains the assumption of its minor toxicity/carcinogenicity potential (Fig. 1 and Fig. 2). Major parameters responsible for the toxicity effects are the small fibre width (W=0.07 μm in Table 3), acicular crystal habit, high fibre density, hydrophilic character, iron content and the rate of iron release. The overall FPTI score is low because of the nanometric size of the fibres (L=0.47 μm in Table 3), absence of silica and no metals other than iron.

4.2.8. Natural halloysite nano-tubes from Matauri Bay, Northern Island (New Zealand)

The evaluated halloysite sample is a commercial "processed" commodity [71] from Matauri Bay (North Island, New Zealand). This product is used in manifold industrial applications. For example, it is

imported in Europe to manufacture glazes for the industry of traditional ceramics. The FPTI score is 1.92 (0.10) (Table 3), in the segment of the negative standards (Fig. 4). The parameter of the model that significantly decreases the overall score is the short fibre size (L=1.5 μm in Table 3) favouring engulfment and clearance of the fibres by alveolar macrophages [17,28]. On the other hand, the very small width (W=0.13 μm in Table 3) plays a key role in toxicity, inflammatory potential and carcinogenicity potential of mineral fibres as it influences pulmonary and pleural deposition depth [17]. The content of iron and metals of the halloysite nano-tubes is very low [33]. Hence, metals driven Fenton primary release of cyto-/geno-toxic hydroxyl radicals, responsible for the toxicity and carcinogenicity of respirable mineral fibres [31], should be minor. Starting from the dissolution data available for kaolinite [72], the calculated dissolution time of halloysite at pH= 4 [33] was 1.18 y, greater than that of non-biodurable chrysotile and much shorter than that of biodurable fibres like amphibole asbestos an erionite [37].

4.2.9. *Synthetic nano-chrysotile*

The synthetic iron-free nano-chrysotile evaluated in this work is described in Lesci et al. [41]. The FPTI score of 1.37 (0.02) (Table 3) is the lowest calculated value and indicates a null toxicity/carcinogenicity potential (Fig. 1 and Fig. 2). The low overall FPTI score is due to the mean fibre length (L=1.0 μm) and the absence of iron and metals which cancels the parameters related to their content and release rates. The null predicted toxicity of this synthetic form of nano-chrysotile confirms the results of *in vitro* testing by Gazzano et al. [22] showing the remarkable inactivity of the synthetic chrysotile in all tests performed on human lung epithelial A549 cells.

4.2.10. *Mordenite from Poona (India)*

The evaluated mordenite is a natural specimen collection quality sample from the zeolite collection of the Chemical and Geological Sciences Department of the University of Modena and Reggio Emilia (Italy). It was collected in the suburbs of Pashan in the Poona district, Maharashtra (India) and was fully characterized by Di Giuseppe [12]. The FPTI score is 2.02 (0.14) (Table 3) within the segment of the negative standards (Fig. 4). Fibre size is a potential toxicity factor because more than 75 % of the fibres are longer than 11 μm and 50 % of the fibres show a width greater than 0.95 μm [12]. Other major toxicity parameters are the acicular crystal habit, the hydrophilic character, the small calculated specific surface area (2.04 m^2/g), and estimated dissolution rate of 200 y. Overall FPTI score is decreased by the negligible content of iron and metals which nullifies the parameters related to their content and release rates.

4.3. *Proposed protocol for the evaluation of mineral fibres*

Fig. 5 reports the flow-chart of a proposed protocol for the evaluation of mineral fibres, showing the role of the FPTI model as preliminary screening tool to predict the fibre potential of toxicity/carcinogenicity. If sporadic epidemiologic data, random *in vivo*, *in vitro*, or mechanistic tests are indicative of possible toxicity/carcinogenicity potential of a mineral fibre, the FPTI model should be applied as preliminary screening tool eventually in combination with other predictive tools such as the EPA *ToxCast*. If the overall FPTI score is within the regions of carcinogenic fibres (see Fig. 3), *in vitro* biomarkers and assays to collect evidence on the 10 KCs [64] should be made. Evidences of the 10 KCs following the IARC evaluation criteria should be eventually followed by specific *in vivo*/mechanistic tests and systematic analysis of the epidemiologic data. With this body of evidence, IARC evaluation process with the results reported in a dedicated IARC Monograph should be planned.

To this aim, a number of relevant mineral fibres wait to be clearly evaluated. Among them fibrous antigorite from New Caledonia [23], fibrous ferrierite form Lovelock (Nevada, USA) [29], and fibrous talc form Gouverneur mining district (NY state, USA) [61] just to list a few fibres not yet or only partly classified to which workers and the population can be potentially exposed to.

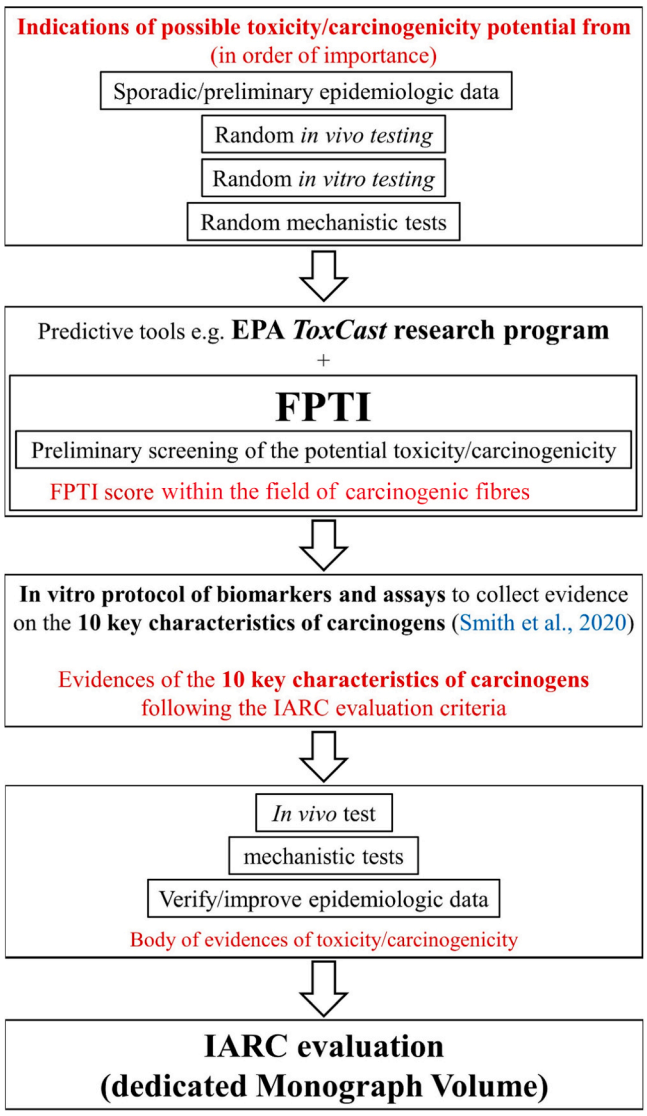

Fig. 5. Proposal of a flow-chart for the evaluation of mineral fibres, highlighting the role of the FPTI model as preliminary screening tool to predict the fibre potential of toxicity/carcinogenicity.

5. Conclusions

The FPTI predictive model serves as innovative advancement in assessing and categorizing mineral fibres based on their potential toxicity and carcinogenicity. Over a decade of research has solidified its role as a screening tool, enabling differentiation between fibres with varying degrees of potential hazardousness.

It was found that distinct classes for amphibole asbestos, chrysotile, erionite, and IARC *Group 3* fibres can be statistically separated with the following rank of potential toxicity/carcinogenicity: amphibole asbestos > erionite > chrysotile. This approach simplifies the preliminary evaluation of mineral fibres and focuses attention on those warranting further investigation.

The importance of parameters such as fibre size, iron/metal content, and dissolution rate in influencing overall toxicity has been evidenced. When integrated with predictive tools like EPA *ToxCast*, FPTI framework offers a comprehensive protocol for risk assessment.

It is important to observe that FPTI is a basic dynamic predictive tool that should be considered open to improvement as the estimation of

some fibre parameters still presents uncertainties related to the limited of knowledge of their role on inducing biological adverse effects and the lack of *in vivo* validation for many fibres. Among the fibre parameters that require further refinement and upgrading are crystal curvature (1,3) and habit (1,4), iron nuclearity (1,10), and cation exchange (1,18).

Moreover, its continued application to emerging fibres of industrial, economic, and social significance ensures relevance in safeguarding public health. With appropriate parameterisation and calibration, the FPTI model may also be applied to emerging nanomaterials or engineered fibres, which are gaining relevance in occupational safety, like carbon (nano)-fibres/tubes or even to fibrous micro-plastics.

The applicative WebFPTI [34] is available online at the link: https://fibers-fpti.unimore.it/FPTI/ and open to test any fibre data.

The statistical analysis allowed the quantitative evaluation of fibres unclassified to date. Fibrous nano-anatase, nano-goethite, calcite and datolite have now been evaluated and resulted to be non-hazardous. Short chrysotile fibres (L≤5μm) also fell outside the class of carcinogenic chrysotiles but above the threshold limit for potentially toxic/carcinogenic fibres.

This methodology supports the global mission of health and environmental institutions in mitigating exposure risks, fostering a proactive stance towards minimizing the adverse effects of hazardous fibres. To this aim, relevant mineral fibres wait to be further evaluated. Among them, fibrous antigorite from New Caledonia, fibrous ferrierite from Lovelock (Nevada, USA), and fibrous talc form Gouverneur mining district (NY state, USA) are examples of mineral fibres partly or not yet classified to which professional and/or environmental exposure is possible.

Environmental implications

This work presents a statistical analysis of the data collected in 10 years with the FPTI predictive model aimed at evaluating the toxicity/carcinogenicity potential mineral fibres. The analysis allowed us to create representative classes of values for amphibole asbestos, chrysotile, erionite, and non-carcinogenic fibres, well-known hazardous agents classified by the IARC) as carcinogens. These classes can be used for the *ab initio* evaluation of mineral fibres of industrial, economic or social importance not classified to date. This work helps addressing environmental problems because it ranks the toxicity and pathogenicity potential of chrysotile, still used worldwide, amphibole asbestos and erionite.

CRediT authorship contribution statement

Mauro Leoncini: Validation, Software, Conceptualization. **Gualtieri Alessandro Francesco:** Writing – review & editing, Writing – original draft, Validation, Methodology, Data curation, Conceptualization.

Declaration of Competing Interest

The authors declare that they have no known competing financial interests or personal relationships that could have appeared to influence the work reported in this paper.

Acknowledgements

This work has been carried out under the project PRIN2022 “SEEDS - Sediments Eco-recycling Exploitation, Development and Sustainability” – Project Code 2022BCL34N, Finanziato dall’Unione europea- Next Generation EU, Missione 4 Componente 1 CUP-E53D23004330006.

Appendix A. Supporting information

Supplementary data associated with this article can be found in the online version at doi:10.1016/j.jhazmat.2025.139202.

Data Availability

Data will be made available on request.

References

[1] Achimovičová, M., Baláž, P., 2008. Kinetics of the leaching of mechanically activated berthierite, boulangerite and franckeite. Phys Chem Miner 35, 95–101.
[2] Baan, R.A., 2007. Carcinogenic hazards from inhaled carbon black, titanium dioxide, and talc not containing asbestos or asbestiform fibers: recent evaluations by an IARC Monographs Working Group. Inhal tox 19 (1), 213–228.
[3] Ballirano, P., Pacella, A., Mirata, S., Passalacqua, M., Di Carlo, M.C., Arrizza, L., Montereali, M.R., Scarfì, S., 2025. Fibrous erionite modifications following THP-1 macrophage phagocytosis: an insight into the mechanisms of interaction with biological systems. J Hazard Mater, 137546.
[4] Bernstein, D.M., Hoskins, J.A., 2006. The health effects of chrysotile: current perspective based upon recent data. Regul Toxicol Pharmacol 45 (3), 252–264.
[5] Bertino, P., Marconi, A., Palumbo, L., Bruni, B.M., Barbone, D., Germano, S., Dogan, A.U., Tassi, G.F., Porta, C., Mutti, L., Gaudino, G., 2007. Erionite and asbestos differently cause transformation of human mesothelial cells. Int J Cancer 121 (1), 12–20.
[6] Bignon, J., Jaurand, M.C., 1983. Biological in vitro and in vivo responses of chrysotile versus amphiboles. Environ Health Perspect 51, 73–80.
[7] Bloise, A., Ricchiuti, C., Punturo, R., Pereira, D., 2020. Potentially toxic elements (PTEs) associated with asbestos chrysotile, tremolite and actinolite in the Calabria region (Italy). Chem Geol 558, 119896.
[8] Cattaneo, A., Somigliana, A., Gemmi, M., Bernabeo, F., Savoca, D., Cavallo, D.M., Bertazzi, P.A., 2012. Airborne concentrations of chrysotile asbestos in serpentine quarries and stone processing facilities in Valmalenco, Italy. Ann Occup Hyg 56 (6), 671–683.
[9] Cornell, R.M., Posner, A.M., Quirk, J.P., 1976. Kinetics and mechanisms of the acid dissolution of goethite (α-FeOOH). J Inorg Nucl Chem 38 (3), 563–567.
[10] Craighead, J.E., 1987. Current pathogenetic concepts of diffuse malignant mesothelioma. Hum Pathol 18 (6), 544–557.
[11] Deng, Q., Wang, X., Wang, M., Lan, Y., 2012. Exposure–response relationship between chrysotile exposure and mortality from lung cancer and asbestosis. Occup Environ Med 69 (2), 81–86.
[12] Di Giuseppe, D., 2020. Characterization of fibrous mordenite: A first step for the evaluation of its potential toxicity. Crystals 10 (9), 769.
[13] Di Giuseppe, D., Harper, M., Bailey, M., Erskine, B., Della Ventura, G., Ardit, M., Pasquali, L., Tomaino, G., Ray, R., Mason, H., Dyar, M.D., Hanuskova, M., Giacobbe, C., Zoboli, A., Gualtieri, A.F., 2019. Characterization and assessment of the potential toxicity/pathogenicity of fibrous glaucophane. Environ Res 178, 108723.
[14] Di Giuseppe, D., Scognamiglio, V., Malferrari, D., Nodari, L., Pasquali, L., Lassinantti Gualtieri, M., Scarfì, S., Mirata, S., Tessari, U., Hanuskova, M., Gualtieri, A.F., 2021. Characterization of fibrous wollastonite NYAD G in view of its use as negative standard for *in vitro* toxicity tests. Minerals 11 (12), 1378.
[15] Di Giuseppe, D., Zoboli, A., Nodari, L., Pasquali, L., Sala, O., Ballirano, P., Malferrari, D., Raneri, S., Hanuskova, M., Gualtieri, A.F., 2021. Characterization and assessment of the potential toxicity/pathogenicity of Russian commercial chrysotile. Am Mineral 106, 1606–1621.
[16] Dogan, A.U., Dogan, M., Hoskins, J.A., 2008. Erionite series minerals: mineralogical and carcinogenic properties. Environ Geochem Health 30, 367–381.
[17] Donaldson, K., Murphy, F.A., Duffin, R., Poland, C.A., 2010. Asbestos, carbon nanotubes and the pleural mesothelium: a review of the hypothesis regarding the role of long fibre retention in the parietal pleura, inflammation and mesothelioma. Part Fibre Toxicol 7, 5–22.
[18] Egilman, D., 2009. Fiber types, asbestos potency, and environmental causation: a peer review of published work and legal and regulatory scientific testimony. Int J Occup Environ Health 15 (2), 202–228.
[19] Feraud, J., Maliqi, G., Meha, V., 2007. Famous Mineral Localities: the Trepca mine, Stari Trg, Kosovo. Mineral Rec 38 (4), 267–299.
[20] Fornasini, L., Raneri, S., Bersani, D., Mantovani, L., Scognamiglio, V., Di Giuseppe, D., Gualtieri, A.F., 2022. Identification of iron compounds in chrysotile from the Balangero mine (Turin, Italy) by micro-Raman spectroscopy. J Raman Spectrosc 53 (11), 1931–1941.
[21] Gangwal, S., Brown, J.S., Wang, A., Houck, K.A., Dix, D.J., Kavlock, R.J., Hubal, E. A.C., 2011. Informing selection of nanomaterial concentrations for ToxCast in vitro testing based on occupational exposure potential. Environ Health persp 119 (11), 1539–1546.
[22] Gazzano, E., Foresti, E., Lesci, I.G., Tomatis, M., Riganti, C., Fubini, B., Roveri, N., Ghigo, D., 2005. Different cellular responses evoked by natural and stoichiometric synthetic chrysotile asbestos. Toxicol Appl Pharmacol 206 (3), 356–364.
[23] Gazzano, E., Petriglieri, J.R., Aldieri, E., Fubini, B., Laporte-Magoni, C., Pavan, C., Tomatis, M., Turci, F., 2023. Cytotoxicity of fibrous antigorite from New Caledonia. Environ Res 230, 115046.
[24] Giacobbe, C., Moliterni, A., Di Giuseppe, D., Malferrari, D., Wright, J.P., Mattioli, M., Raneri, S., Giannini, C., Fornasini, L., Mugnaioli, E., Ballirano, P., Gualtieri, A.F., 2023. The crystal structure of the killer fibre erionite from Tuzköy (Cappadocia, Turkey). IUCrJ 10 (4).

[25] Gianfagna, A., Andreozzi, G.B., Ballirano, P., Mazziotti-Tagliani, S., Bruni, B.M., 2007. Structural and chemical contrasts between prismatic and fibrous fluoro-edenite from Biancavilla, Sicily, Italy. Can Mineral 45 (2), 249–262.
[26] Gualtieri, A.F., 2018. Towards a quantitative model to predict the toxicity/pathogenicity potential of mineral fibers. Toxicol Appl Pharm 361, 89–98.
[27] Gualtieri, A.F., 2021. Bridging the gap between toxicity and carcinogenicity of mineral fibres by connecting the fibre crystal-chemical and physical parameters to the key characteristics of cancer. Curr Res Toxicol 2, 42–52.
[28] Gualtieri, A.F., 2023. Journey to the centre of the lung. The perspective of a mineralogist on the carcinogenic effects of mineral fibres in the lungs. J Hazard Mater 442, 130077. https://doi.org/10.1016/j.jhazmat.2022.130077.
[29] Gualtieri, A.F., Bursi Gandolfi, N., Passaglia, E., Pollastri, S., Mattioli, M., Giordani, M., Ottaviani, M.F., Cangiotti, M., Bloise, A., Barca, D., Vigliaturo, R., Viani, A., Pasquali, L., Gualtieri, M.L., 2018. Is fibrous ferrierite a potential health hazard? Characterization and comparison with fibrous erionite. Am Mineral 103 (7), 1044–1055.
[30] Gualtieri, A.F., Bursi Gandolfi, N., Pollastri, S., Pollok, K., Langenhorst, F., 2016. Where is iron in erionite? A multidisciplinary study on fibrous erionite-Na from Jersey (Nevada, USA). Sci Rep 6 (1), 37981.
[31] Gualtieri, A.F., Cocchi, M., Muniz-Miranda, F., Pedone, A., Castellini, E., Strani, L., 2024. Iron nuclearity in mineral fibres: unravelling the catalytic activity for predictive modelling of toxicity. J Hazard Mater 469, 134004.
[32] Gualtieri, A.F., Di Giuseppe, D., 2022. Letter to the Editor: comments on the paper of Wylie and Korchevskiy – Carcinogenicity of fibrous glaucophane: how should we fill the data gaps?. In: Current Research in Toxicology, 3, 100063.
[33] Gualtieri, A.F., Glossop, L., Malferrari, D., Castellini, E., Gualtieri, M.L., Hanuskova, M., Nodari, L., Ogor, J., Fantini, R., 2025. Evaluation of the potential toxicity of respirable commercial halloysite elongate mineral particles (EMPs). Appl Clay Sci.
[34] Gualtieri, A.F., Leoncini, M., Rinaldi, L., Zoboli, A., Di Giuseppe, D., 2021. WebFPTI: A tool to predict the toxicity/pathogenicity of mineral fibres including asbestos. Earth Sci Inform 14 (4), 2401–2409.
[35] Gualtieri, A.F., Lusvardi, G., Zoboli, A., Di Giuseppe, D., Lassinantti Gualtieri, M., 2019. Biodurability and release of metals during the dissolution of chrysotile, crocidolite and fibrous erionite. Environ Res 171, 550–557.
[36] Gualtieri, A.F., Mossman, B.T., Roggli, V.L., 2017. Towards a general model for predicting the toxicity and pathogenicity of mineral fibres. Mineral Fibres: Crystal Chemistry, Chemical-Physical Properties, Biological Interaction and Toxicity. European Mineralogical Union-EMU Notes in Mineralogy, London, pp. 501–532.
[37] Gualtieri, A.F., Pollastri, S., Gandolfi, N.B., Lassinantti Gualtieri, M., 2018. *In vitro* acellular dissolution of mineral fibres: a comparative study. Sci Rep 8 (1), 1–12.
[38] Kosmulski, M., Durand-Vidal, S., Mączka, E., Rosenholm, J.B., 2004. Morphology of synthetic goethite particles. J Colloid Interface Sci 271 (2), 261–269.
[39] Krewski, D., Bird, M., Al-Zoughool, M., Birkett, N., Billard, M., Milton, B., Rice, J. M., Grosse, Y., Cogliano, V.J., Hill, M.A., Baan, R.A., Little, J., Zielinski, J.M., 2019. Key characteristics of 86 agents known to cause cancer in humans. J Tox Environ Health Part B 22, 244–263.
[40] Kumar, G.S., Girija, E.K., Thamizhavel, A., Yokogawa, Y., Kalkura, S.N., 2010. Synthesis and characterization of bioactive hydroxyapatite–calcite nanocomposite for biomedical applications. J Colloid Interface Sci 349 (1), 56–62.
[41] Lesci, I.G., Balducci, G., Pierini, F., Soavi, F., Roveri, N., 2014. Surface features and thermal stability of mesoporous Fe doped geoinspired synthetic chrysotile nanotubes. Microporous Mesoporous Mater 197, 8–16.
[42] Maltoni, C., Minardi, F., Morisi, L., 1982. Pleural mesotheliomas in Sprague-Dawley rats by erionite: first experimental evidence. Environ Res 29 (1), 238–244.
[43] Maltoni, C., Minardi, F., 1989. Recent results of carcinogenicity bioassays of fibres and other particulate materials. In: Non-occupational exposure to mineral fibers, 90. IARC Scientific Publications, pp. 46–53, 1989.
[44] Mbanga, O., Cukrowska, E., Gulumian, M., 2022. Dissolution of titanium dioxide nanoparticles in synthetic biological and environmental media to predict their biodurability and persistence. Toxicol Vitr 84, 105457.
[45] McDonald, J.C., McDonald, A.D., 1996. The epidemiology of mesothelioma in historical context. Eur Respir J 9 (9), 1932–1942.
[46] McDonald, J.C., McDonald, A.D., 1997. Chrysotile, tremolite and carcinogenicity. The. Ann Occup Hyg 41 (6), 699–705.
[47] Moëlo, Y., Makovicky, E., Mozgova, N.N., Jambor, J.L., Cook, N., Pring, A., Paar, W., Nickel, E.H., Graeser, S., Karup-Møller, S., Balic-Žunic, T., Mumme, W.G., Vurro, F., Topa, D., Bindi, L., Bente, K., Shimizu, M., 2008. Sulfosalt systematics: a review. Report of the sulfosalt sub-committee of the IMA Commission on Ore Mineralogy. Eur J Mineral 20 (1), 7–46.
[48] Moore, D.S., McCabe, G.P., 1999. Introduction to the Practice of Statistics, Third ed. W.H. Freeman, New York.
[49] Mossman, B.T., Gualtieri, A.F., 2020. Lung cancer: Mechanisms of carcinogenesis by asbestos. In chapter 12 occupational cancers, Second ved. Springer, pp. 239–256.
[50] Okazaki, Y., 2022. Asbestos-induced mesothelial injury and carcinogenesis: Involvement of iron and reactive oxygen species. Pathol Int 72 (2), 83–95.
[51] Pacella, A., Andreozzi, G.B., Ballirano, P., Gianfagna, A., 2008. Crystal chemical and structural characterization of fibrous tremolite from Ala di Stura (Lanzo Valley, Italy). Per Miner 77 (2), 51–62.
[52] Pacella, A., Andreozzi, G., Nodari, L., Ballirano, P., 2019. Chemical and structural characterization of UICC crocidolite fibres from Koegas Mine, Northern Cape (South Africa). Period di Mineral 88 (3), 297–306.
[53] Palekar, L.D., Eyre, J.F., Most, B.M., Coffin, D., 1987. Metaphase and anaphase analysis of V79 cells exposed to erionite, UICC chrysotile and UICC crocidolite. Carcinogenesis 8 (4), 553–560.
[54] Papa, E., Dearden, J.C., Gramatica, P., 2007. Linear QSAR regression models for the prediction of bioconcentration factors by physicochemical properties and structural theoretical molecular descriptors. Chemosphere 67 (2), 351–358.
[55] Patel, J.P., Brook, M., Kah, M., Hamilton, A., Gamberini, M.C., Zoboli, C., Mugnaioli, E., Malferrari, D., Fantini, R., Arletti, R., Gualtieri, A.F., 2024. Characterization and potential toxicity of asbestiform erionite from Gawler Downs, New Zealand. Am Mineral 109 (9), 1499–1512.
[56] Pollastri, S., Gualtieri, A.F., Gualtieri, M.L., Hanuskova, M., Cavallo, A., Gaudino, G., 2014. The zeta potential of mineral fibres. J Hazard Mater 276, 469–479.
[57] Pollastri, S., Perchiazzi, N., Gigli, L., Ferretti, P., Cavallo, A., Bursi Gandolfi, N., Pollok, K., Gualtieri, A.F., 2017. The crystal structure of mineral fibres. 2. Amosite and fibrous Anthophyllite. Period di Mineral 86 (2017), 55–65.
[58] Pollastri, S., Perchiazzi, N., Lezzerini, M., Plaisier, J.R., Cavallo, A., Dalconi, M.C., Bursi Gandolfi, N., Gualtieri, A.F., 2016. The crystal structure of mineral fibres. 1. Chrysotile. Period di Mineral 85, 249–259.
[59] Poole, A., Brown, R.C., Turver, C.J., Skidmore, J.W., Griffiths, D.M., 1983. *In vitro* genotoxic activities of fibrous erionite. Br J Cancer 47 (5), 697–705.
[60] Raneri, S., Gianoncelli, A., Bonanni, V., Mirata, S., Scarfì, S., Fornasini, L., Bersani, D., Baroni, D., Picco, C., Gualtieri, A.F., 2024. The influence of cation exchange on the possible mechanism of erionite toxicity: a synchrotron-based micro-X-ray fluorescence study on THP-1-derived macrophages exposed to erionite-Na. Environ Res 252, 118878.
[61] Ross, M., Smith, W.L., Ashton, W.H., 1968. Triclinic talc and associated amphiboles from Gouverneur mining district, New York. Am Mineral 53 (5–6), 751–769.
[62] Scarfì, S., Almonti, V., Mirata, S., Passalacqua, M., Vernazza, S., Patel, J.P., Brook, M., Hamilton, H., Kah, M., Gualtieri, A.F., 2025. *In vitro* cyto-and geno-toxicity of asbestiform erionite from New Zealand. Environ Res 265, 120415.
[63] Scognamiglio, V., Di Giuseppe, D., Lassinantti Gualtieri, M., Tomassetti, L., Gualtieri, A.F., 2021. A systematic study of the cryogenic milling of chrysotile asbestos. Appl Sci 11, 4826.
[64] Smith, M.T., Guyton, K.Z., Kleinstreuer, N., Borrel, A., Cardenas, A., Chiu, W.A., Felsher, D.W., Gibbons, C.F., Goodson, W.H., Houck, K.A., Kane, A.B., La Merrill, M.A., Lebrec, H., Lowe, L., McHale, C.M., Minocherhomji, S., Rieswijk, L., Sandy, M.S., Sone, H., Wang, A., Zhang, L., Zeise, L., Fielden, M., 2020. The key characteristics of carcinogens: relationship to the hallmarks of cancer, relevant biomarkers, and assays to measure them. Cancer Epidemiol Biomark Prev 29 (10), 1887–1903.
[65] Stayner, L.T., Dankovic, D., Lemen, R., 1996. Occupational exposure to chrysotile asbestos and cancer risk: a review of the amphibole hypothesis. Am J Public Health 86 (2), 179–186.
[66] Suzuki, Y., 1980. Carcinogenic and fibrogenic effects of zeolites: preliminary observations. Environ Res 27, 433–445.
[67] Tian, L., Wang, L., Wang, K., Zhang, Y., Liang, J., 2019. The preparation and properties of porous sepiolite ceramics. Sci Rep 9 (1), 7337.
[68] Tóth, G., Hermann, T., Da Silva, M.R., Montanarella, L., 2016. Heavy metals in agricultural soils of the European Union with implications for food safety. Environ Int 88, 299–309.
[69] U.S. Environmental Protection Agency (EPA), 2012. USEPA T. E. S. T. Tool, User's Guide for T.E.S.T.
[70] Wagner, J.C., Berry, G., Pooley, F.D., 1982. Mesotheliomas and asbestos type in asbestos textile workers: a study of lung contents. Br Med J (Clin Res Ed) 285 (6342), 603–606.
[71] Wilson, I., Keeling, J., 2016. Global occurrence, geology and characteristics of tubular halloysite deposits. Clay Miner 51 (3), 309–324.
[72] Yang, L., Steefel, C.I., 2008. Kaolinite dissolution and precipitation kinetics at 22C and pH 4. Geochim Et Cosmochim Acta 72 (1), 99–116.
[73] Yang, W. (1990). *Solubilities of selected borosilicate minerals between 25 degrees and 250 degrees Celcius and P (V)= P (water)*. Washington State University.
[74] Zaccarini, F., Morales-Ruano, S., Scacchetti, M., Garuti, G., Heide, K., 2008. Investigation of datolite (CaB [SiO4/(OH)]) from basalts in the Northern Apennines ophiolites (Italy): genetic implications. Geochemistry 68 (3), 265–277.